



Monte Carlo simulation of SiPMs with GATE

Brahim Mehadji, Mathieu Dupont, Denis Fougeron, Christian Morel

► To cite this version:

Brahim Mehadji, Mathieu Dupont, Denis Fougeron, Christian Morel. Monte Carlo simulation of SiPMs with GATE. 2023. hal-03791752

HAL Id: hal-03791752

<https://hal.science/hal-03791752>

Preprint submitted on 23 Mar 2023

HAL is a multi-disciplinary open access archive for the deposit and dissemination of scientific research documents, whether they are published or not. The documents may come from teaching and research institutions in France or abroad, or from public or private research centers.

L'archive ouverte pluridisciplinaire **HAL**, est destinée au dépôt et à la diffusion de documents scientifiques de niveau recherche, publiés ou non, émanant des établissements d'enseignement et de recherche français ou étrangers, des laboratoires publics ou privés.

Monte Carlo simulation of SiPMs with GATE

Brahim Mehadji,^{1,*} Mathieu Dupont,¹ Denis Fougeron¹ and Christian Morel¹

¹*Aix-Marseille Univ, CNRS/IN2P3, CPPM, Marseille, France*

**present address: Aix Marseille Univ, APhM, Hôpital de la Timone et Nord, Radiothérapie, Marseille, France*

E-mail: mehadji@cppm.in2p3.fr

ABSTRACT: Silicon photomultipliers (SiPMs) replace photomultiplier tubes (PMTs) for the detection of light in many applications, particularly in high energy physics and medical imaging. We describe a flexible implementation of a SiPM model for the GATE Monte Carlo simulation platform, which is based on the SiPM noise description proposed by Rosado and Hidalgo, and describe an easy and effective method to determine and instantiate the SiPM noise model with simple measurements. We also simulate the micro-cell Single Photon Time Resolution (SPTR) and describe its measurement.

KEYWORDS: Monte Carlo simulation, GATE, SiPM

Contents

1	Introduction	1
2	Collecting SiPM properties for their simulation with GATE	2
2.1	Shape of the micro-cell signal	2
2.2	White noise	2
2.3	Recovery time constant and noise distributions	4
2.3.1	Recovery time constant	4
2.3.2	Crosstalk probabilities	5
2.3.3	Dark Count Rate (DCR)	6
2.3.4	After-pulse time distribution	6
2.3.5	Delayed-crosstalk time distribution	7
2.4	Single Photon Time Resolution (SPTR)	8
3	Setting up the SiPM simulation in GATE	10
3.1	The SiPM.XML file	10
3.1.1	The Surfaces.XML instantiating	11
3.1.2	Writing macros	11
4	Validation of the SiPM signal generation	12
5	Conclusion	13
A	SiPM.XML	14
B	Surfaces.XML	15

1 Introduction

Silicon photomultipliers (SiPMs) replace photomultiplier tubes (PMTs) for the detection of light in many applications, particularly in high energy physics and medical imaging [1] [2] [3]. A SiPM is composed of thousands of micro avalanche photodiodes [4]. Their sizes vary from one to tens of millimeters depending on the SiPM model. The detection of an optical photon by one micro avalanche photodiode (also called micro-cell) induces an electric signal (pulse). The SiPM signal corresponds to the sum of all the pulses issued by the micro-cells. This signal is very sensitive to temperature and over-voltage [5]. This involves various sources of noise, which basically consist in dark counts (a random firing of a micro-cell due to thermic excitation), crosstalks (micro-cells that fire due to infrared excitation resulting from the avalanche of another neighbor micro-cell), after-pulses (a micro-cell that fires again a few nanoseconds after the bulk interaction resulting from

a first avalanche within the micro-cell), delayed-crosstalks (a micro-cell that fires a few nanoseconds after the bulk interaction resulting from a first avalanche in another micro-cell) and white noise.

Two types of SiPMs are currently available on the market, digital SiPMs (dSiPMs) and analog SiPMs (aSiPMs). The main difference between dSiPMs and aSiPMs is that dSiPMs include a signal digitizing part whereas aSiPMs do not. While dSiPMs have already been modelled in GATE [6], aSiPMs have only been modelled with GEANT4 [7].

We present a flexible implementation of aSiPM in GATE [8] [9] instantiating all the SiPM noise sources described above. For this, we implement the noise description proposed by Rosado and Hidalgo in [10] and use an easy and effective method to determine and instantiate SiPM noise sources with simple measurements. We also simulate the micro-cell Single Photon Time Resolution (SPTR) and describe its measurement.

2 Collecting SiPM properties for their simulation with GATE

As it will be described in Section 3, the Monte Carlo simulation of SiPM with GATE requires to instantiate a number of SiPM specifications. Some of them are provided by the manufacturer, e.g., the number of micro-cells or the SiPM size, and some are not and need to be determined experimentally. Following [10], we describe a method to measure the micro-cell pulse shape and recovery time constant, the SiPM Dark Count Rate (DCR) and crosstalk probabilities, and the after-pulse and delayed-crosstalk time distributions by acquiring the signal of the SiPM placed in the dark. The micro-cell SPTR is determined by illuminating the SiPM with an attenuated picosecond laser. The method is exemplified with an SiPM HPK MPPC S13360-3050.

2.1 Shape of the micro-cell signal

The pulse generated at t_0 by a micro-cell can be described by a double exponential characterized by a rising time constant τ_{rise} , a falloff time constant τ_{fall} and an amplitude C_{amp} as expressed by Eq. 2.1, where $h(t - t_0)$ is the Heaviside function. To determine those constants, micro-cell pulses must be acquired with the SiPM placed in the dark (Figure 1).

$$A = C_{\text{amp}} \times h(t - t_0) \times \left(1 - e^{-\frac{t-t_0}{\tau_{\text{rise}}}}\right) \times e^{-\frac{t-t_0}{\tau_{\text{fall}}}} \quad (2.1)$$

Since the amplitude C_{amp} can vary from one micro-cell to another and from one pulse to another, it is important to analyze several pulses corresponding to the detection of one photon (i.e., generating only one micro-cell pulse) and to determine the standard deviation on the estimation of C_{amp} . For the SiPM placed in the dark, we measured $C_{\text{amp}} = 5.01 \pm 0.29$ mV.

For simulations aiming to study the time resolution of an SiPM, the approximation of a micro-cell pulse by a double exponential function is not enough accurate. One should rather proceed to a signal sampling with an appropriate sampling period given the time resolution of the spectrometric chain (i.e., < 50 ps for a typical SiPM SPTR of 100 ps).

2.2 White noise

White noise is characterized by its standard deviation, which is determined on the SiPM signal in absence of pulse. For the SiPM, we measure a standard deviation of 0.377 mV.

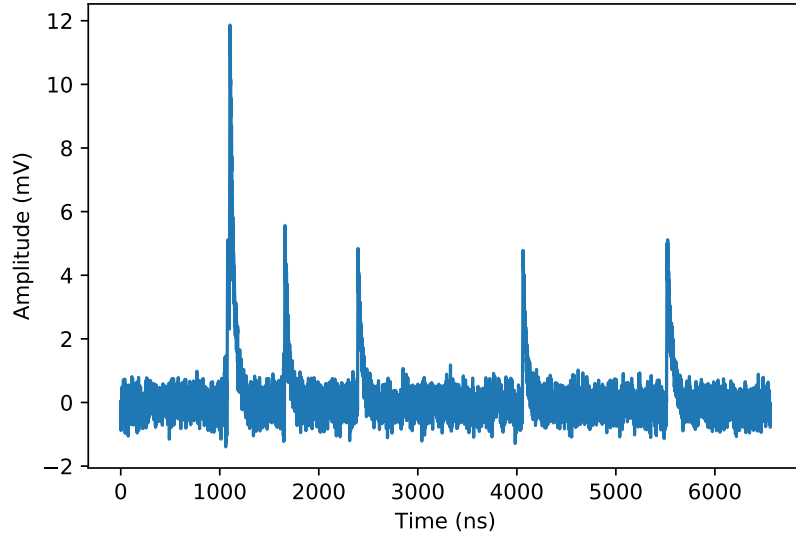


Figure 1. A $6.5\,\mu\text{s}$ time frame of the signal originated from the SiPM placed in the dark. Pulses of equal amplitudes correspond to individual micro-cell dark counts.

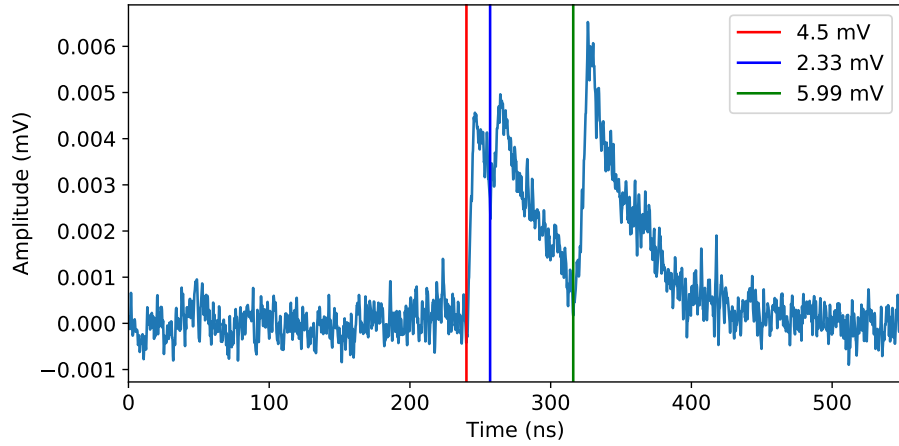


Figure 2. Time frame of a typical signal originated from the SiPM placed in the dark comprising a dark count (the first pulse called primary), one after-pulse (the second pulse) and probably one delayed-crosstalk (the last pulse). Pulses starting times are indicated with vertical lines and corresponding amplitudes are presented in the legend.

2.3 Recovery time constant and noise distributions

Using time frames of the SiPM signal acquired in the dark, one can notice that some pulses are correlated. For example, in Figure 2, three pulses are visible. Presumably, the first pulse is a dark count and the two other pulses following it are correlated with it. By measuring the amplitudes and the time delays from the first pulse, which is called primary, we can infer that the second pulse is an after-pulse because its amplitude is lower than the amplitude of the primary, i.e., the micro-cell has not restored completely at the time of the second pulse, and the third pulse is a delayed-crosstalk because its amplitude is similar to the amplitude of the primary. The steps of the method proposed by Rosado and Hidalgo [10] to determine the micro-cell recovery time constant, the SiPM DCR and crosstalk probabilities, and the after-pulse and delayed-crosstalk time distributions are listed below:

1. Measuring SiPM signal frames in dark conditions.
2. Deconvolve the signal shape given by Eq. 2.1 from the SiPM signal frames sampled in the dark.
3. Using the deconvolved signal, find pulses with an amplitude at least three times higher than the white noise standard deviation.
4. Using signal frames, determine the amplitudes using the "peakdet" function available in python [11] with a threshold three times higher than the white noise standard deviation and compute the amplitude from the minimum to the maximum value of the leading edge.
5. Whenever no pulse is observed in the signal frame for 500 ns, the next pulse with an amplitude higher than $C_{\text{amp}} - 3 \times \sigma_{C_{\text{amp}}}$ is considered as a primary pulse with $\sigma_{C_{\text{amp}}}$ the standard deviation of C_{amp} .
6. Using signal frames, determine the time delays from the primary pulse of pulses following it within 500 ns, which are thus considered as correlated.
7. For these correlated pulses, plot a 2D histogram of amplitudes versus time delays from the primaries.

Figure 3 presents a 2D histogram of amplitudes versus time delays from the primaries obtained by analyzing 1000 signal frames from the SiPM with a duration of 3.2 ms. The SiPM was placed in the dark at a temperature of 21 °C and was biased with an over-voltage of 3 V ($V = V_{\text{br}} + 3$ where V_{br} is the micro-cell breakdown voltage). Its signal was amplified by a gain of 21.

2.3.1 Recovery time constant

When a micro-cell fires, it takes a few nanoseconds to recover. Hence, when a micro-cell fires, and then again a few nanoseconds later with a time delay t from the primary, i.e., corresponding to the occurrence of an after-pulse, the amplitude of the micro-cell signal $C_{\text{amp}}(t)$ follows Eq. 2.2 where τ_{rec} is the recovery time constant of the micro-cell. It is then estimated by fitting with Eq. 2.2 the rising part of the lower branch of the 2D histogram (Figure 4).

For this, time delay slices of 1 ns were projected on the amplitude axis. A gaussian fit was then performed on every amplitude profile and a fit of Eq. 2.2 on their mean weighted by their standard

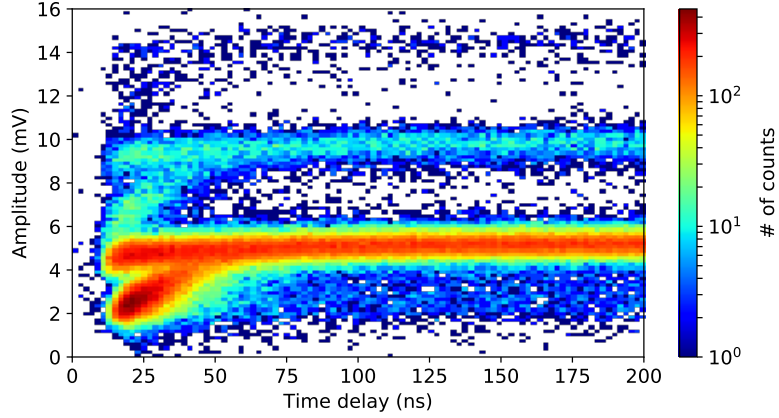


Figure 3. 2D histogram of amplitudes versus time delays from primaries measured for the SiPM placed in the dark.

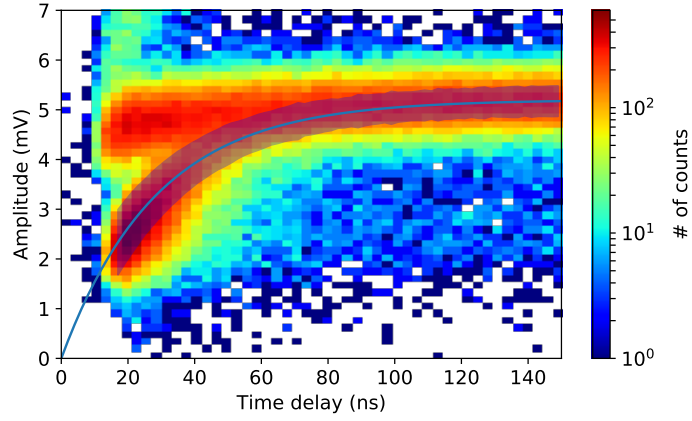


Figure 4. 2D histogram of amplitudes versus time delays from primaries measured for the SiPM placed in the dark with (in blue) the mean amplitudes and standard deviations fitted on amplitude profiles binned within 1 ns time slices.

deviation as a function of the time delay t returns the recovery time constant τ_{rec} with its error. In our case, τ_{rec} amounts to 28.5 ± 0.5 ns.

$$C_{\text{amp}}(t) = C_{\text{amp}} \times \left(1 - e^{-\frac{t}{\tau_{\text{rec}}}}\right) \quad (2.2)$$

2.3.2 Crosstalk probabilities

Pulses occurring between 100 and 500 ns after the primaries were selected and projected on the amplitude axis (Figure 5 left). In those conditions, only few after-pulses remain and their impact on the estimation of the probability of crosstalk is negligible.

Several peaks are visible on the amplitude projection (Figure 5 right), which correspond to pulses with 0, 1, 2, 3 or 4 crosstalks. Gaussian fits were performed on each peak, whose integrals estimate the number of events observed with 0 up to 4 crosstalks. The crosstalk probabilities (up to 4 crosstalks) listed in Table 1 are obtained by dividing the integral of the gaussian fits by the number

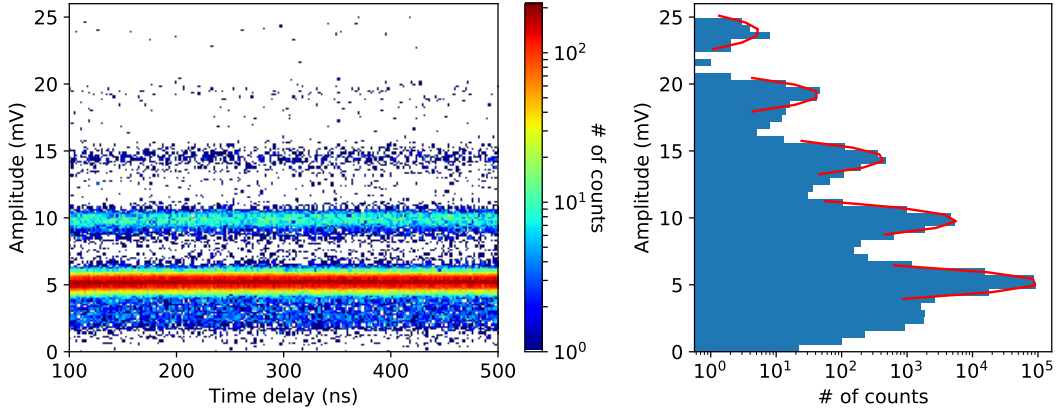


Figure 5. (left) 2D histogram of amplitudes versus time delays from primaries measured for the SiPM placed in the dark and (right) its amplitude projection with (in red) gaussian fits on peaks centred approximately on 5, 10, 15, 20 and 25 mV corresponding to pulses with 0, 1, 2, 3 and 4 crosstalks, respectively.

of events measured between 100 ns and 500 ns. The amplitudes recorded below 5 mV correspond to uncorrelated afterpulses, mostly correlated to dark counts which appear during the 500 ns time delay.

The crosstalk probability ϵ_c , i.e., the probability to have at least one crosstalk, is defined as one minus the probability to have no crosstalks and amounts to 5.4%.

Table 1. Probability of the number of crosstalks (CT)

0 CT [%]	1 CT [%]	2 CT [‰]	3 CT [‰]	4 CT [‰]
94.6 ± 1.3	4.9 ± 0.1	3.9 ± 0.2	3.7 ± 0.3	0.5 ± 0.1

2.3.3 Dark Count Rate (DCR)

In the 2D histogram, pulses occurring 200 ns after the primary are considered as uncorrelated. Pulses are projected onto the time delay axis, re-binned within 1 ns time delay intervals and divided by the number of primaries (1 193 132). The DCR is computed as the mean value of bins (Figure 6). A DCR of 498 ± 2.9 kHz was obtained.

2.3.4 After-pulse time distribution

In [10], Rosado and Hidalgo model the after-pulse time distribution $P_{AP}(t)$ with the equation:

$$P_{AP}(t) = C_{AP} \times \left(1 - e^{-\frac{t}{\tau_{rec}}}\right) \times t^a \times e^{-\frac{t}{\tau_{bulk}}} \times k(t) \quad (2.3)$$

where t represents the time delay from the primary. C_{AP} is a constant which corresponds to the probability that an after-pulse occurs at $t = 0$. τ_{bulk} is the minority carrier lifetime in the silicon substrate, which is also called bulk lifetime. The function $k(t)$ allows to estimate the number of pulses that are not detected because their amplitude is smaller than the amplitude of the electric

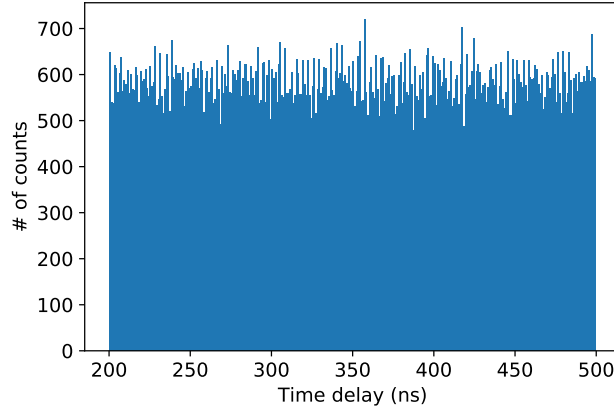


Figure 6. Time delay projection of pulses binned within 1 ns time intervals

noise. The factor t^a is an ad hoc dependency set by the authors to reproduce the observed data with $a = -1$.

Hence, we used pulses selected so that $k(t) = 1$ with amplitudes smaller than 4.1 mV that appear at least 20 ns after the primary to fit the after-pulse time distribution (Figure 7) with the function:

$$A \times \left(1 - e^{-\frac{t}{\tau_{\text{rec}}}}\right) \times \frac{1}{t} \times e^{-\frac{t}{\tau_{\text{bulk}}}} \quad (2.4)$$

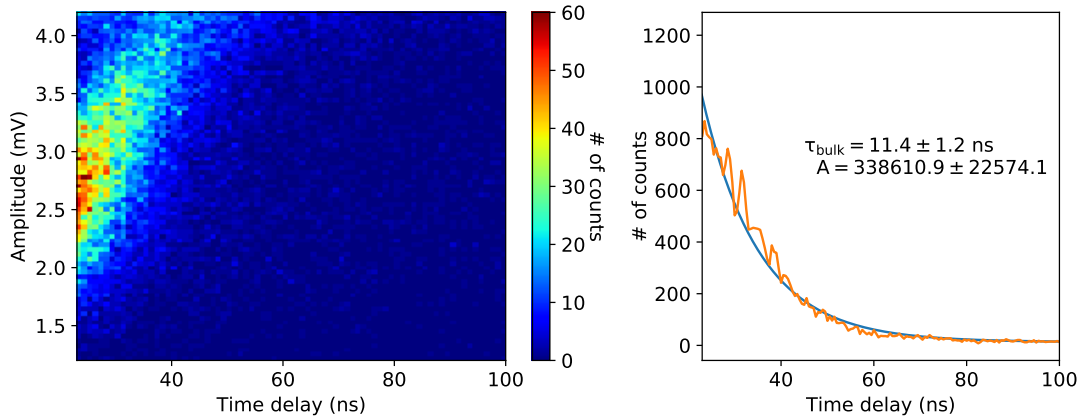


Figure 7. (left) 2D histogram of amplitudes versus time delays from primaries measured for the SiPM placed in the dark and (right) its time delay projection (in orange) used to fit (in blue) Eq. 2.4 to estimate τ_{bulk} and C_{AP} .

The amplitude C_{AP} of the after-pulse time distribution is then obtained by dividing A by the number of primaries (1 193 132) and by the probability to have no crosstalks $1 - \epsilon_c$. The estimations of τ_{bulk} and C_{AP} are $\tau_{\text{bulk}} = 11.4 \pm 1.2$ ns and $C_{\text{AP}} = 0.30 \pm 0.02$, which are in concordance with the values presented by Rosado and Hidalgo in [10].

2.3.5 Delayed-crosstalk time distribution

In [10], Rosado and Hidalgo model the delayed-crosstalk time distribution $P_{\text{CT}}(t)$ with the equation:

$$P_{\text{CT}}(t) = C_{\text{CT}} \times t^b \times e^{-\frac{t}{\tau_{\text{bulk}}}} \quad (2.5)$$

where, t represents the time delay from the primary, and C_{CT} is a constant expressed in unit of $[\text{time}]^{-1/2}$. The factor t^b is an ad hoc factor set by the authors to reproduce the measured distribution with $b = -1/2$.

We used pulses with amplitudes between 4.2 mV and 6 mV to fit the delayed-crosstalk time distribution (Figure 8) with the function:

$$A \times \frac{1}{\sqrt{t}} \times e^{-\frac{t}{\tau_{\text{bulk}}}} + \text{DCR} \times (\# \text{ primaries}) \quad (2.6)$$

where τ_{bulk} is set to 11.4 ns. Indeed, dark counts are also present and must be taken into account by an offset in the fit given by $\text{DCR} \times (\# \text{ primaries})$. A few delayed-pulses are also present in this region, but their contribution to the delayed-crosstalk time distribution was considered negligible.

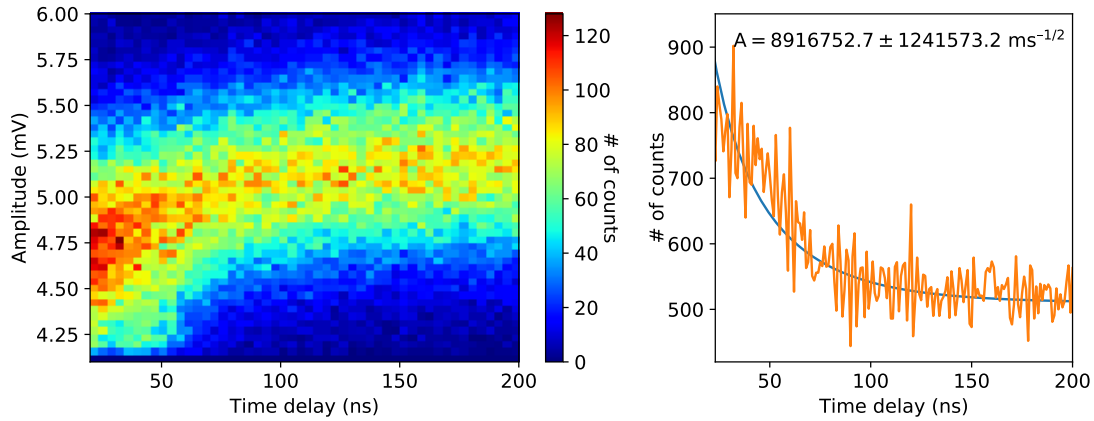


Figure 8. (left) 2D histogram of amplitudes versus time delays from primaries measured for the SiPM placed in the dark and (right) its time delay projection (in orange) used to fit (in blue) Eq. 2.6 in order to estimate C_{CT} .

The amplitude C_{CT} of the delayed-crosstalk time distribution is then obtained by dividing A by the number of primaries (1 193 132) and by the probability to have no crosstalks $1 - \epsilon_c$. It amounts to $7.9 \pm 1.2 \text{ ms}^{-1/2}$.

2.4 Single Photon Time Resolution (SPTR)

To measure the SPTR, we used the amplification electronic setup proposed by Cates et al. [12][13]. This setup allows to get a very good signal to noise ratio owing to the differential measurement of the SiPM signal and the use of an inductance with a ratio 1 : 1 that provides a passive amplification of the signal.

The SiPM was biased with an over-voltage of 9 V and illuminated with a laser pulse of 20 ps FWHM. The fiber output was placed 50 cm away from the SiPM face and we used an attenuating iris followed by a diverging lens to shape the light pulse so as that only one photon impinges onto the surface of the SiPM (Figure 9).

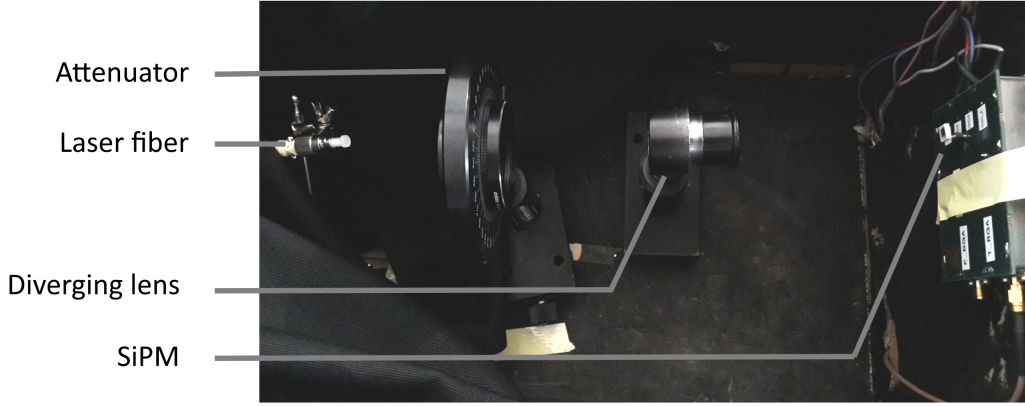


Figure 9. Picture of the experimental setup used to measure the SPTR.

An oscilloscope sampled the signal at 40 GHz during 300 ns each time the signal was triggered above a fixed amplitude over noise. Figure 10 shows the histogram of the time difference between the laser pulse and the trigger. As described by E. Grushka et al. in [14], we used a convolution between a gaussian distribution and an exponential decay distribution given by the expression:

$$f(t; \mu, \sigma, \lambda) = \frac{1}{\sqrt{2\pi}\sigma} \times e^{-\frac{(t-\mu)^2}{2\sigma^2}} * \lambda e^{-\lambda t} \quad (2.7)$$

to fit this histogram. The standard deviation of the gaussian distribution amounts to $\sigma_{\text{measured}} = 136 \pm 20$ ps FWHM. Note that this value is in concordance with the measurement of Cates *et al.* performed in similar conditions (SiPM type, over-voltage, amplification circuit, and fit function) [12]. It also comprises the resolutions of the oscilloscope trigger, the laser ($\sigma_{\text{laser}} = 20$ ps FWHM), and the electronic noise.

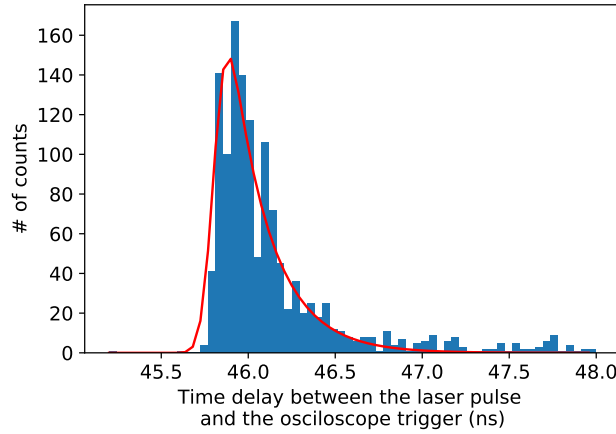


Figure 10. Histogram of the time difference between the laser pulse and the trigger with (in red) the result of the fit of Eq. 2.7.

To estimate the resolution of the trigger, a sharp signal was duplicated and measured simultaneously on two different channels of the oscilloscope. The histogram of the time difference between

the two trigger signals allowed to estimate the resolution of the oscilloscope trigger, which amounts to $\sigma_{\text{trigger}} = (31 \pm 0.6)/\sqrt{2} = 21.9 \pm 0.4$ ps FWHM.

The electronic noise contribution can be estimated by measuring the FWHM of the white noise divided by the SiPM signal slope at the trigger position. It amounts to $\sigma_{\text{elec}} = 43.4 \pm 0.3$ ps FWHM.

The SPTR of the SiPM is then expressed by:

$$\text{SPTR} = \sqrt{\sigma_{\text{measured}}^2 - \sigma_{\text{trigger}}^2 - \sigma_{\text{laser}}^2 - \sigma_{\text{elec}}^2} = 125.4 \pm 21.4 \text{ ps FWHM} \quad (2.8)$$

at $V_{\text{ov}} = 9$ V and is in agreement with other measurements available in the literature [15].

As proposed by Acerbi et al. in [15], the micro-cell SPTR is modeled in GATE by adding to the pulse start time t_0 a randomized time following a gaussian distribution centered on 0.

3 Setting up the SiPM simulation in GATE

Three files need to be modified or created in order to simulate an SiPM in GATE:

- The file `SiPM.XML` for the parameters of the SiPM signal generation.
- A file for simulation with the extension `.mac`, which contains the macros allowing to provide the SiPM geometry.
- The file `Surfaces.XML` for the SiPM surface and Photon Detection Efficiency (PDE) definitions.

3.1 The `SiPM.XML` file

Many types of SiPMs with different properties can be defined in this file. An example is presented in Appendix A in which one can find:

- `deadTime`: Mean dead time of a micro-cell
- `tauRecovery`: Mean recovery time of a micro-cell (τ_{rec})
- `SPTR`: Single Photon Time Resolution
- `tauBulk`: Bulk lifetime (τ_{bulk})
- `Cap`, `Cct`, `a` and `b` are the constants C_{AP} , C_{CT} , a and b of Eq 2.3 and 2.5 used to describe the time distributions of after-pulses and delayed-crosstalks, respectively
- `signalDeconvolvedAmplitude`: Mean amplitude of a pulse
- `durationPulse`: Desired time duration of a generated pulse (more than $3 \times \tau_{\text{fall}}$ is recommended)
- `signalDeconvolvedAmplitudeSigma`: Pulse amplitude standard deviation
- `whiteNoiseSigma`: White noise standard deviation
- `DCR`: Dark Count Rate

- **Dimensions:** Dimensions of one micro-cell
- **CROSSTALK:** Probabilities of the number of crosstalks (0, 1, 2, etc.)
- **CROSSTALK DISPERSION:** Spatial dispersion of crosstalks and delayed-crosstalks (the first line represents the probability that the closest micro-cells fire, the second line represents the probability that micro-cells at a double distance fire, and so forth)
- **Pulse:** Mean signal sampled for one firing micro-cell (its duration must be superior or equal to *durationPulse*)

3.1.1 The Surfaces.XML instantiating

This file contains the reflectance and PDE of the SiPM. Explanations about each part of this xml file can be found in reference [16]. Many types of surfaces can be described. As an illustration, we chose to create one type with the name SiPM in Appendix B. In this example, the SiPM surface is polished. Therefore, the values of SPECULARLOBECONSTANT, SPECULARSPIKECONSTANT, BACKSCATTERCONSTANT and sigmaalpha are set to zero. The SiPM micro-cells are placed behind an optical coating (epoxy, glass, etc.). The SiPM surface is then defined as polished and composed by a dielectric material with the reflectance of silicon (REFLECTIVITY) measured by Green and Keevers in [17]. Last but not least, EFFICIENCY stores the PDE of the SiPM provided by the manufacturer.

3.1.2 Writing macros

A new parallelepiped object named SiPM with its dimensions and composition is created in the file with the extension .mac as follows:

```
1 /gate/world/daughters/name SiPM
2 /gate/world/daughters/insert box
3 /gate/SiPM/geometry/setXLength 1.2 mm
4 /gate//geometry/setYLength 3.4 mm
5 /gate/SiPM/geometry/setZLength 3.4 mm
6 /gate/SiPM/setMaterial Epoxy
```

where Epoxy sets the composition of the SiPM surface, which leads to use the refraction index of Epoxy for optical photon tracking in the Monte Carlo simulation. Then, digitizer named sipm of type SiPM is inserted as follows:

```
1 /gate/digitizer/Singles/insert sipm
2 /gate/digitizer/Singles/sipm/setVolume SiPM_params
3 /gate/digitizer/Singles/sipm/type SiPM
4 /gate/digitizer/Singles/sipm/setStartSignal 0 s
5 /gate/digitizer/Singles/sipm/setDurationSignal 3 s
6 /gate/digitizer/Singles/sipm/setStepSignal 0.2 ns
7 /gate/digitizer/Singles/sipm/surface YZ
8 /gate/digitizer/Singles/sipm/initialize
```

where `setVolume` sets the parameters of `sipm` to the parameters registered with the name `SiPM_params` in the file `SiPM.xml`. In this example, the signal duration amounts to 3 s and contains one value every 0.2 ns. The orientation of the SiPM detection surface is set within the (y,z) plane.

When the SiPM is defined directly in the «world», the type of surface encountered by photons coming from the world that are impinging onto the SiPM surface and vice versa are defined by:

```
1 /gate/world/surfaces/name SiPMToworld
2 /gate/world/surfaces/insert SiPM
3 /gate/world/surfaces/SiPMToworld/setSurface SiPM_surface
4
5 /gate/SiPM/surfaces/name worldToSiPM
6 /gate/SiPM/surfaces/insert world
7 /gate/SiPM/surfaces/worldToSiPM/setSurface SiPM_surface
```

which makes `sipm` ready for the simulation. The results are stored in numpy format, which is readable by the numpy python module [18]. The signals and pulses generated by `sipm` are contained in the files `signal.npy` and `pulse.npy`, respectively.

4 Validation of the SiPM signal generation

To verify the correct instantiating of the SiPM parameters and signal generation, we have simulated prompt micro-cell discharges that mimic the DCR generated by an SiPM placed in the dark (i.e., in absence of light or radioactive sources). The SiPM parameters that are instantiated in the simulation are those measured in Section 2. The 2D histogram of amplitudes versus time delays from primaries obtained for simulated data is displayed in Figure 11. This histogram is indeed quite similar to the measurements presented in the Figure 3, though it is noticeably less noisy because the measured noise is not a pure white noise in contrary to the noise simulated with GATE. The Tables 2 and 3 present a comparison of the parameters estimated on the measured and simulated data following the methodology described in Section 2. The measured parameters and their estimations on simulated data all agree within their uncertainties, which validates both the implementation of the SiPM model and the methodology used to estimate these parameters.

Relative uncertainties on the probabilities of the number of crosstalks amounts to 0.5%, 1.6%, 7.8%, 25.5% and 40% for 0 to 4 crosstalks, respectively. Indeed, these relative errors become rather large above 2 crosstalks, but the sum of their probabilities can almost be neglected and amounts to 12.5‰, i.e., 1.5% of the probability to have one or two crosstalks.

Table 2. Comparison between the measured noise parameters defined in `SiPM.XML` (see Appendix A) and their estimations on simulated data.

	C_{AP}	C_{CT} [ms ^{-1/2}]	DCR [kHz]	τ_{rec} [ns]	τ_{bulk} [ns]
measurement	0.30 ± 0.02	7.9 ± 1.2	498 ± 2.9	28.5 ± 0.5	11.4 ± 1.2
simulation	0.28 ± 0.02	7.2 ± 2.4	502 ± 2.8	28.5 ± 0.8	11.2 ± 1.3

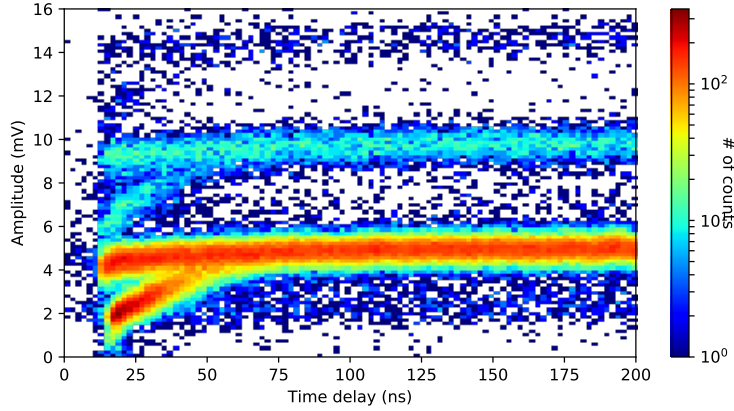


Figure 11. 2D histogram of amplitudes versus time delays from primaries simulated for the SiPM placed in the dark.

Table 3. Comparison between the measured probabilities of the number of crosstalks defined in SiPM.XML (see Appendix A) and their estimations on simulated data.

	0 CT [%]	1 CT [%]	2 CT [‰]	3 CT [‰]	4 CT [‰]
measurement	91.0 ± 0.5	7.9 ± 0.1	9.0 ± 0.7	1.1 ± 0.3	1.5 ± 0.6
simulation	91.0 ± 0.5	8.2 ± 0.2	9.9 ± 0.7	1.3 ± 0.4	1.8 ± 0.8

5 Conclusion

A Monte Carlo model of SiPM based on the noise description proposed by Rosado and Hidalgo in [10] was developed for GATE. It implements the generation of dark counts, crosstalks, after-pulses, delayed-crosstalks and white noise with parameters instantiated from dedicated xml files. These SiPM parameters need to be defined for a specific gain, temperature and over voltage, and can be determined experimentally by using a laser pulse to estimate the micro-cell SPTR and by recording dark counts with the SiPM placed in the dark.

The GATE implementation of the noise model described by Rosado and Hidalgo was verified by simulating prompt micro-cell discharges that mimic the DCR generated by an SiPM placed in the dark and by comparing the parameters estimated on the simulated data following the methodology presented in Section 2. The agreement between the parameters instantiated in GATE and their estimations on simulated data validates both the implementation of the SiPM model and the methodology used to estimate these parameters.

In a further work, we will present a comparison of the measured and simulated data from a scintillation crystal read out by an SiPM and study the impact of the various SiPM sources of noise on the time and energy resolutions of this spectrometric chain.

Acknowledgements

We thank Jaime Rosado for helpful discussions about his SiPM noise description. This work was supported by the project TEMPORAL funded by the ANDRA/PIA under the grant No. RTSC-

NADAA160019.

A SiPM.XML

```
1 <?xml version="1.0" encoding="utf-8"?>
2 <sipms>
3   <sipm name="SiPM">
4     <propertystable>
5       <property name="tauRecovery" value="28.5" unit="nanosecond"/>
6       <property name="tauBulk" value="11.4" unit="nanosecond"/>
7       <property name="sptr" value="125.4" unit="picosecond"/>
8       <property name="Cap" value="0.030"/>
9       <property name="Cct" value="0.0079"/>
10      <property name="t0" value="0." unit="nanosecond"/>
11      <property name="a" value="-1."/>
12      <property name="b" value="-0.5"/>
13      <property name="signalDeconvolvedAmplitude" value="0.0048" unit="volt"/>
14      <property name="durationPulse" value="300" unit="nanosecond"/>
15      <!-- Duration of one pulse generated by one micro-cell-->
16      <property name="signalDeconvolvedAmplitudeSigma" value="0.00025" unit="volt"/>
17      <property name="whiteNoiseSigma" value="3.77E-04" unit="volt"/>
18      <property name="DCR" value="498" unit="kilohertz"/>
19      <propertyvector name="DIMENSIONS" unit="micrometer">
20        <ve value="50."></ve>
21        <ve value="50."></ve>
22      </propertyvector>
23      <!-- Dimentions of one micro-cell-->
24      <propertyvector name="CROSSTALK">
25        <ve value="9.1e-01"></ve>
26        <ve value="7.90e-02"></ve>
27        <ve value="9.00e-03"></ve>
28        <ve value="1.10-03"></ve>
29        <ve value="1.46e-04"></ve>
30      </propertyvector>
31      <propertyvector name="CROSSTALK_DISPERSION">
32        <ve value="1"></ve>
33      </propertyvector>
34      <!-- Set to 1 means that all micro-cells at a distance from center to center of the
          firing micro-cell equal to 50 micrometers have the same probability to create a
          crosstalk. Then, each new line in the vector is a circle of bigger radius (50
          micrometers) where we can define the probability of crosstalk for all the micro-
          cells that it passes through. The sum of the vector is equal to 1.-->
35      <propertyvector name="PULSE" unit="nanosecond">
36        <ve time="0.00" value="0.011675983255"></ve>
37        <ve time="0.05" value="0.014392492543"></ve>
38        [...]
39      </propertyvector>
40    </propertystable>
41  </sipm>
42 </sipms>
```

. SiPM.XML

B Surfaces.XML

```
1 <?xml version="1.0" encoding="utf-8"?>
2 <surfaces>
3   <surface name="SiPM" type="dielectric_metal" sigmaalpha="0.0" finish="polished">
4     <propertytable>
5       <propertyvector name="SPECULARLOBECONSTANT" energyunit="eV">
6         <ve energy="1.0" value="0.0"></ve>
7         <ve energy="2.34" value="0.0"></ve>
8         <ve energy="4.13" value="0.0"></ve>
9       </propertyvector>
10      <propertyvector name="SPECULARSPIKECONSTANT" energyunit="eV">
11        <ve energy="1.0" value="0.0"></ve>
12        <ve energy="2.34" value="0.0"></ve>
13        <ve energy="4.13" value="0.0"></ve>
14      </propertyvector>
15      <propertyvector name="BACKSCATTERCONSTANT" energyunit="eV">
16        <ve energy="1.0" value="0.0"></ve>
17        <ve energy="2.34" value="0.0"></ve>
18        <ve energy="4.13" value="0.0"></ve>
19      </propertyvector>
20      <propertyvector name="REFLECTIVITY" energyunit="eV">
21        <ve energy="4.9592" value="0.672612594017585"></ve>
22        <ve energy="4.76846153846154" value="0.705173999753657"></ve>
23        <ve energy="4.59185185185185" value="0.732089552684876"></ve>
24        <ve energy="4.42785714285714" value="0.722956410931167"></ve>
25        <ve energy="4.2751724137931" value="0.684235361230538"></ve>
26        <ve energy="4.13266666666667" value="0.623487589028101"></ve>
27        <ve energy="3.99935483870968" value="0.590475835158614"></ve>
28        <ve energy="3.874375" value="0.574130337860842"></ve>
29        <ve energy="3.7569696969697" value="0.5656774122022"></ve>
30        <ve energy="3.64647058823529" value="0.561749318208869"></ve>
31        <ve energy="3.54228571428571" value="0.565380275909807"></ve>
32        <ve energy="3.44388888888889" value="0.582911002404122"></ve>
33        <ve energy="3.35081081081081" value="0.584270801263058"></ve>
34        <ve energy="3.26263157894737" value="0.546502292447187"></ve>
35        <ve energy="3.17897435897436" value="0.510973643823881"></ve>
36        <ve energy="3.0995" value="0.486021027692078"></ve>
37        <ve energy="3.02390243902439" value="0.466853259650879"></ve>
38        <ve energy="2.95190476190476" value="0.451521580514202"></ve>
39        <ve energy="2.88325581395349" value="0.439123248850964"></ve>
40        <ve energy="2.81772727272727" value="0.428907265346926"></ve>
41        <ve energy="2.75511111111111" value="0.419585699502722"></ve>
42        <ve energy="2.69521739130435" value="0.411485950400365"></ve>
43        <ve energy="2.63787234042553" value="0.404281394203058"></ve>
44        <ve energy="2.58291666666667" value="0.39787918076254"></ve>
45        <ve energy="2.53020408163265" value="0.391964732835764"></ve>
46        <ve energy="2.4796" value="0.387105531276213"></ve>
47        <ve energy="2.43098039215686" value="0.382264521501647"></ve>
48        <ve energy="2.38423076923077" value="0.377999091926155"></ve>
49        <ve energy="2.33924528301887" value="0.374142013737281"></ve>
50        <ve energy="2.29592592592593" value="0.370428522192012"></ve>
```

```

51 <ve energy="2.25418181818182" value="0.367335936121879"></ve>
52 <ve energy="2.21392857142857" value="0.364216221196157"></ve>
53 <ve energy="2.17508771929825" value="0.361451748594409"></ve>
54 <ve energy="2.13758620689655" value="0.358667134606895"></ve>
55 <ve energy="2.10135593220339" value="0.356344975212093"></ve>
56 <ve energy="2.06633333333333" value="0.354106671849336"></ve>
57 <ve energy="2.03245901639344" value="0.351853614251938"></ve>
58 <ve energy="1.99967741935484" value="0.349785241326916"></ve>
59 <ve energy="1.96793650793651" value="0.34820133857332"></ve>
60 <ve energy="1.9371875" value="0.346411479932793"></ve>
61 <ve energy="1.90738461538462" value="0.344713928379056"></ve>
62 <ve energy="1.87848484848485" value="0.34330931640043"></ve>
63 <ve energy="1.85044776119403" value="0.341798625402933"></ve>
64 <ve energy="1.82323529411765" value="0.340281901015896"></ve>
65 <ve energy="1.7968115942029" value="0.338962422361468"></ve>
66 <ve energy="1.77114285714286" value="0.337639001584691"></ve>
67 <ve energy="1.74619718309859" value="0.336413284699118"></ve>
68 <ve energy="1.72194444444444" value="0.3352856253833"></ve>
69 <ve energy="1.69835616438356" value="0.3342575899929"></ve>
70 <ve energy="1.67540540540541" value="0.33332999879242"></ve>
71 <ve energy="1.65306666666667" value="0.332400672745742"></ve>
72 <ve energy="1.63131578947368" value="0.331468651680362"></ve>
73 <ve energy="1.61012987012987" value="0.330534830393574"></ve>
74 <ve energy="1.58948717948718" value="0.329598359402392"></ve>
75 <ve energy="1.56936708860759" value="0.328764393207925"></ve>
76 <ve energy="1.54975" value="0.328032867790877"></ve>
77 <ve energy="1.53061728395062" value="0.327300305896179"></ve>
78 <ve energy="1.5119512195122" value="0.326671301461493"></ve>
79 <ve energy="1.49373493975904" value="0.326041006227035"></ve>
80 <ve energy="1.47595238095238" value="0.32540997581366"></ve>
81 <ve energy="1.45858823529412" value="0.324777930560902"></ve>
82 <ve energy="1.44162790697674" value="0.324144649551891"></ve>
83 <ve energy="1.42505747126437" value="0.323510569194358"></ve>
84 <ve energy="1.40886363636364" value="0.322875469350817"></ve>
85 <ve energy="1.39303370786517" value="0.3222391901263"></ve>
86 <ve energy="1.37755555555556" value="0.321602046138182"></ve>
87 <ve energy="1.36241758241758" value="0.320963878059092"></ve>
88 <ve energy="1.34760869565217" value="0.320324684364472"></ve>
89 <ve energy="1.33311827956989" value="0.319684463534747"></ve>
90 <ve energy="1.31893617021277" value="0.319150063811936"></ve>
91 <ve energy="1.30505263157895" value="0.318615045243477"></ve>
92 <ve energy="1.29145833333333" value="0.318079310589019"></ve>
93 <ve energy="1.27814432989691" value="0.317542858980053"></ve>
94 <ve energy="1.26510204081633" value="0.317113180903694"></ve>
95 <ve energy="1.25232323232323" value="0.316683042980187"></ve>
96 <ve energy="1.2398" value="0.316252444768591"></ve>
97 </propertyvector>
98 <propertyvector name="EFFICIENCY" energyunit="eV">
99 <ve energy="3.85914154653" value="0.0254237288136"></ve>
100 <ve energy="3.77987804878" value="0.0656779661017"></ve>
101 <ve energy="3.68526282854" value="0.122881355932"></ve>
102 <ve energy="3.57779465371" value="0.176906779661"></ve>

```

```

103     <ve energy="3.50956495828" value="0.224576271186"></ve>
104     <ve energy="3.30474186308" value="0.278601694915"></ve>
105     <ve energy="3.19016793066" value="0.333686440678"></ve>
106     <ve energy="2.98330800405" value="0.372881355932"></ve>
107     <ve energy="2.81234479465" value="0.396186440678"></ve>
108     <ve energy="2.6792766151" value="0.400423728814"></ve>
109     <ve energy="2.5582319722" value="0.39406779661"></ve>
110     <ve energy="2.32401341752" value="0.353813559322"></ve>
111     <ve energy="2.23239196361" value="0.317796610169"></ve>
112     <ve energy="2.10473552538" value="0.271186440678"></ve>
113     <ve energy="1.99628813559" value="0.235169491525"></ve>
114     <ve energy="1.87429980904" value="0.185381355932"></ve>
115     <ve energy="1.77916918429" value="0.156779661017"></ve>
116     <ve energy="1.67017867272" value="0.118644067797"></ve>
117     <ve energy="1.56707025013" value="0.0879237288136"></ve>
118     <ve energy="1.49392440386" value="0.0646186440678"></ve>
119     <ve energy="1.37916861827" value="0.0370762711864"></ve>
120   </propertyvector>
121 </propertiestable>
122 </surface>
123 </surfaces>

```

. Surfaces.XML

References

- [1] T. Lewellen, *Recent developments in PET detector technology*, *Phys. Med. Biol.* **53** (2008) R287.
- [2] M. Conti and B. Bendriem, *The new oportunities for high time resolution clinical TOF PET*, *Clin. Transl. Imaging* **7** (2019) 139.
- [3] V. Kovaltchouk et al., *Comparison of a silicon photomultiplier to a traditional vacuum photomultiplier*, *Nucl. Instrum. Meth. A* **538** (2005) 408.
- [4] D. Renker and E. Lorenz, *Advances in solid state photon detectors*, *J. Instrum.* **4** (2009) P04004.
- [5] O. Adam Nepomuk et al., *Characterization of Three High Efficiency and Blue Sensitive Silicon Photomultipliers*, *Nucl. Instrum. Meth. A* **846** (2017) 106.
- [6] J. Salvadori et al., *Monte Carlo simulation of digital photon counting PET*, *EJNMMI Physics* **7** (2020) 23.
- [7] T. Niggemann, *G4SiPM: A novel silicon photomultiplier simulation package for Geant4*, *Nucl. Instrum. Meth. A* **787** (2015) 344.
- [8] S. Jan et al., *GATE: a simulation toolkit for PET and SPECT*, *Phys. Med. Biol.* **49** (2004) 4543.
- [9] S. Jan et al., *GATE V6: a major enhancement of the GATE simulation platform enabling modelling of CT and radiotherapy*, *Phys. Med. Biol.* **56** (2011) 881.
- [10] J. Rosado and S. Hidalgo, *Characterization and modeling of crosstalk and afterpulsing in Hamamatsu silicon photomultipliers*, *J. Instrum* **10** (2015) 10031.
- [11] E. Billauer, "Peak detection in python." <https://gist.github.com/endolith/250860>, 2011.
- [12] J. Cates et al., *Improved single photon time resolution for analog SiPMs with front end readout that reduces influence of electronic noise*, *Phys. Med. Biol.* **63** (2018) 185022.

- [13] s. Gundacker et al., *High-frequency SiPM readout advances measured coincidence time resolution limits in TOF-PET*, *Phys. Med. Biol.* **64** (2019) 055012.
- [14] E. Grushka et al., *Characterization of exponentially modified Gaussian peaks in chromatography*, *Anal. Chem.* **42** (1972) 1733–.
- [15] F. Acerbi and S. Gundacker, *Understanding and simulating SiPMs*, *Nucl. Instrum. Meth. A* **926** (2019) 16.
- [16] “GATE users guide.” <http://www.opengatecollaboration.org>, 2018.
- [17] M. A. Green and M. J. Keevers, *Optical properties of intrinsic silicon at 300 K*, *Prog. Photovoltaics* **3** (1995) 189.
- [18] “Python Software Foundation. Python Language Reference, version 3.” <https://www.python.org/>, 2021.